PAN
ARCHIVES OF ACOUSTICS
Vol. **44**, No. 4, pp. 659–668 (2019)
DOI: 10.24425/aoa.2019.129722

The Forces Driving Streaming in the Presence of Scatterers Mimicking the Blood Cells and the Contrast Agents

Janusz WÓJCIK*, Wojciech SECOMSKI, Norbert ŻOŁEK

Department of Ultrasound
Institute of Fundamental Technological Research
Polish Academy of Sciences
Pawińskiego 5B, 02-106 Warsaw, Poland
e-mail: {wsecom, nzolek}@ippt.pan.pl
*Corresponding Author e-mail: jwojcik@ippt.pan.pl

(*received May 24, 2019; accepted September 17, 2019*)

Acoustical Driving Forces (ADF), induced by propagating waves in a homogeneous and inhomogeneous lossy fluid (suspension), are determined and compared depending on the concentration of suspended particles. Using integral equations of the scattering theory, the single particle (inclusion) ADF was calculated as the integral of the flux of the momentum density tensor components over the heterogeneity surface. The possibility of negative ADF was indicated. Originally derived, the total ADF acting on inclusions only, stochastically distributed in ambient fluid, was determined as a function of its concentration. The formula for the relative increase in ADF, resulting from increased concentration was derived. Numerical ADF calculations are presented. In experiments the streaming velocities in a blood-mimicking starch suspension (2 μm radius) in water and Bracco BR14 contrast agent (SF6 gas capsules, 1 μm radius) were measured as the function of different inclusions concentration. The source of the streaming and ADF was a plane 2 mm diameter 20 MHz ultrasonic transducer. Velocity was estimated from the averaged Doppler spectrum obtained from originally developed pulsed Doppler flowmeter. Numerical calculations of the theoretically derived formula showed very good agreement with the experimental results.

Keywords: streaming suspension; scattering; acoustical driving force; Doppler measurements; contrast agents.

1. Introduction

In lossy homogenous fluid streaming results from non elastic momentum transfer through acoustic (potential) mode to a fluid (Eckart, 1948). This transfer is described by the Acoustical Driving Force (ADF_h) which depends only on absorption and intensity of sound. Viscous forces resist the flow. The balance between both forces manifests in the stationary flow. In multi-phase medium, meaning suspension, the asymmetry in forward-backward scattering of the sound on solid or fluid inclusions generate additional components of ADF, which affect the streaming speed (equilibrium speed). Scientific and practical importance phenomena in the range of ADF (or acoustical radiation pressure) and streaming result from the fact that enable testing and influences on the thermo-mechanical properties of matter and non-contact mass and energy flow control such as acoustic levitation, containerless processing, filtration and selection of molecules etc. The possible medical applications of high-frequency-induced ADF were investigated in terms of influencing the movement of blood cells, thrombi, transport control of microcapsules and ultrasound contrast agents in blood vessels to increase the efficiency of thrombolytic and diagnostic therapies. Wu and Du (1993) and Tjotta (1959) showed that in a lossy homogeneous medium, the axial component of the streaming speed v_z is described by the Poisson equation $\eta\Delta v_z = (1/c)\partial_z I_z$, where $\mathrm{ADF}_h := (1/c)\partial_z I_z$. From the other side: $\mathrm{ADF}_h \cong -(2a/\eta c)I_z$. Variables η, c, a are kinematic shear viscosity, speed of sound and absorption coefficient respectively, I_z is the axial component of the sound intensity vector, here ADF_h denotes the density of Acoustical Driving Force in homogenous fluid. The right hand side terms give the ADF_h per unit mas. The numerical solutions of this equation for the acoustic Gaussian beam presented by

Wu and Du (1993) and Nowicki *et al.* (1997; 1998) agreed well with the experiment. There is a number of motion models of multi-phase media (suspensions) in the literature. The most advanced ones include the works of Zhang and Prosperetti (1994; 1997) in which the motion of the continuous phase (surrounding fluid) and dispersion (heterogeneities) are described by conjugated equations. None of these models explicitly considered the acoustic mod. Explicitly its "inclusion" in the existing palette of interactions further increases the level of complexity. There are simplifications used to avoid viscosity (in real fluids an important factor driving the continuous phase).

In publications, ADF is determined for a single fixed molecule. If the results of tracking of the motion that it generates are presented, that this is a movement of a single material point (see Lei *et al.*, 2013). There are no equations, generalizing the above, describing the global stationary movement of the suspension as a "one-fluid" heterogeneous medium.

In this work we show a method of transition from the description, the point of ADF action to a set of inhomogeneities stochastically distributed in ambient fluid to a continuous, dependent on the concentration of heterogeneity, description of the resultant ADF action on the fluid element. Although we do not analyze the effects of "secondary" stresses generated by stationary flow on the heterogeneities of viscosity, in our opinion the presented method is the first step to generalize the description of Wu and Du (1993) and Tjotta (1959) to a hypothetical form $\eta\Delta v_z = (\mathrm{ADF}_h) + (\mathrm{ADF}) + (sec.eff \propto \nabla\eta)$. The streaming velocity v_z results with equilibrium between sum of driving forces $(\mathrm{ADF}_h) + (\mathrm{ADF})$ and the viscous resistance force $\eta\Delta v_z$. For this reason, the main goals of the work were:

1) determining the ratio $\varepsilon := \mathrm{ADF}/\mathrm{ADF}_h$ as a function of the concentration of heterogeneity (ADF increments as a function of concentration);
2) experimental determination of streaming speed increments (equilibrium speed) as a function of concentration of inclusions and comparison of both values.

To determine the ADF acting on a single inclusions, it is necessary to determine the scattered field. For this purpose, we use the integral equation of the scattering theory. This is an original and effective approach, especially when we can use a single scattering approximation. We use it because in our experiments the ratio of heterogeneity radius (1–2 μm) to wavelength (75 μm) was small enough. Literature uses fields in the form of expansions into infinite series. More broadly this issue is discussed further in the text. Although the presented method is not limited by the shape of inclusions, we apply it to spherical heterogeneities. An example of one of the first works devoted to the determination of ADF and the accompanying torque for a different shape (infinite thin cylinder) – and with the use of field distribution into infinite series, is the work of Czyż and Gudra (1992).

Due to the need to carry out accurate measurements of changes in the speed of streaming in the reference medium and in the scope of low concentration of inclusions, the original pulsed Doppler flowmeter operating at 20 MHz frequency was used. Also due to the scope of the experiment's parameters, the presented work covers an area not exposed in the literature.

2. Basic equations and assumptions

In this section we use normalized system of dependent and independent variables. The dimensional variables and operators are accentuated. The normalization was performed as follows. The normalized coordinates in space and time are $\mathbf{x} := K_0'\mathbf{x}'$; $t := \Omega_0' t'$, whereas $\nabla := \nabla'/K_0'$ is the normalized nabla vector operator and $\partial_t := \partial_{t'}/\Omega_0'$ is the derivation operator with respect to time. The characteristic wave number K_0' and pulsation Ω_0' are restricted by the relations: $K_0' c_0' = \Omega_0'$ and $\Omega_0' := 2\pi/T_0'$, where T_0' is the reference time (e.g. time window). The normalized pulsation (frequency) and the wave number in dispersion-less media are equal to $\omega := \omega'/\Omega_0'$ and $k_0(\omega) = \pm\omega$, respectively. For Fourier series representations of the disturbances, ω is discrete variable (integer) which enumerates the components of the series. Normalized density and speed of sound are given by $\widetilde{g} = \widetilde{g}(\mathbf{x}, t) := \widetilde{g}(\mathbf{x}, t)'/g_0'$, $g = g(\mathbf{x}) := g'/g_0'$, respectively, and $c = c(\mathbf{x}) := c'/c_0'$, g_0' and c_0' are density and speed of sound in reference medium (in our case – volume dominant reference). This means that $g = g_0 = 1$ and $c = c_0 = 1$ for reference medium. The pressure and vector of the velocity field are normalized as follows: $\widetilde{P} := \widetilde{P}'/P_0'$, $\boldsymbol{\upsilon} := \boldsymbol{\upsilon}'/v_0'$; $q := v_0'/c_0' = P_0'/g_0' c_0'^2$ is the Mach number, P_0' is the pressure amplitude of the disturbance source. The distribution of the absorption coefficients is normalized as follows $a(\omega, \mathbf{x}) := a'(\omega'/\Omega_0', \mathbf{x})/K_0'$.

Despite the normalization, we retained the symbolism of size, which, after normalization, assumes the value of 1, as for example $g_0 = 1$, $c_0 = 1$. In this way, these formulas retain the structure of standard ones, which makes it easier to give them a physical dimension and identification with the standard ones used in the literature.

We use Euler's description of the medium in which the primary fields $\widetilde{g}(\mathbf{x}, t)$ and $\boldsymbol{\upsilon}(\mathbf{x}, t)$ are evolving in time according to

$$\partial_t \widetilde{g} + q\nabla \cdot \widetilde{g}\boldsymbol{\upsilon} = 0, \tag{1}$$

$$\partial_t \widetilde{g}\boldsymbol{\upsilon} + q\nabla \circ \widetilde{g}\boldsymbol{\upsilon}\boldsymbol{\upsilon} = \nabla \circ \boldsymbol{\Pi}, \tag{2}$$

$$\nabla \circ \boldsymbol{\Pi} := -\nabla \widetilde{P}(\widetilde{g}, \boldsymbol{\upsilon}) - \eta\nabla \times \nabla \times \boldsymbol{\upsilon}, \tag{3}$$

$$\widetilde{P}(\widetilde{g},\boldsymbol{\upsilon}) := gc^2\left[(\widetilde{g}/g)^{\gamma}-1\right]\big/q\gamma + 2gc\,\boldsymbol{\mathcal{A}}^{v}\boldsymbol{\upsilon}, \qquad (4)$$

where $\boldsymbol{\Pi}$ is the stress tensor in dissipative medium (viscous, relaxing, heat conducting), $\widetilde{g}\boldsymbol{\upsilon}\boldsymbol{\upsilon}$ is the Reynolds stress tensor, $\widetilde{P}(\widetilde{g},\boldsymbol{\upsilon})$ is the potential mode pressure. The nearly adiabatic transition of the medium was assumed; γ is the exponent of the adiabate, $\boldsymbol{\mathcal{A}}^{v}$ is the convolution type operator describing the dissipation (Wójcik, Gambin, 2017). For classic viscous media $\boldsymbol{\mathcal{A}}^{v} := \alpha_2\nabla\cdot$, $\alpha_2 := (4\eta_s'/3+\eta_b'+(\gamma-1)\kappa'/c_p')\cdot K_0'/2c_0'$; η_s', η_b', κ', c_p' are, respectively, kinematic coefficients of shear and bulk viscosity, heat conduction and specific heat. $\eta := K_0'^2\eta_s'/\Omega_0'$ is the normalized sear viscosity, $\eta = K_0'^2/|k_s'|^2 = (K_0'\delta_s')^2/2 = q/\mathrm{Re}_0$, $k_s' := (1+i)/\delta_s'$, $\delta_s' := \sqrt{2\eta_s'/\Omega_0'}$ is the acoustical boundary layer thickness, Re_0 – Reynolds number for the scale $1/K_0'$.

In Euler coordinates, Acoustical Radiation Force (ARF) acting on the volume ϑ of the medium, bounded by the constant in time surface S, is determined based on the formula

$$\mathbf{F} := \int_{\vartheta}\nabla\circ\langle\boldsymbol{\Pi}-q\widetilde{g}\boldsymbol{\upsilon}\boldsymbol{\upsilon}\rangle\,\mathrm{d}\vartheta = \int_{s}\langle\boldsymbol{\Pi}-q\widetilde{g}\boldsymbol{\upsilon}\boldsymbol{\upsilon}\rangle\circ\mathbf{n}\,\mathrm{d}s, \quad (5)$$

where Eq. (5) is usually determined only on the basis of acoustic variables (see e.g. Settnes, Bruus, 2012; Mitri, 2012; Zarembo, Krasilnikow, 1966). $\langle\cdot\rangle := \int_{t}^{t+T}(\cdot)/T$ is an average over period of disturbance or repetition time T, $\mathbf{n}$ is the unit outward normal to the surface S. The ADF is defined by Eq. (5) in which the term $\widetilde{g}\boldsymbol{\upsilon}\boldsymbol{\upsilon}$ is neglected. The term ADF is used to emphasize the fact that in Eq. (5) we temporarily disregard the Reynolds stress tensor $\widetilde{g}\boldsymbol{\upsilon}\boldsymbol{\upsilon}$ describing the inertial reaction of the medium to $\boldsymbol{\Pi}$. We are interested in the basic effect of the acoustic field as an external factor that can control the movement of the suspension. For an incompressible or poorly compressible medium, it is often assumed $(\boldsymbol{\upsilon}\boldsymbol{\upsilon})\circ\mathbf{n} = \boldsymbol{\upsilon}(\boldsymbol{\upsilon}\cdot\mathbf{n}) = \mathbf{0}$. ARF and ADF differ in constant factors, which in our case leads to negligible differences between them. Nevertheless, in the further, numerical part of the work, we give an equation taking into account the influence of the omitted component, i.e. the transition from ADF to ARF. In this way, in addition to shortening the considerations, we obtain a comparison of both forces.

We assume that $\boldsymbol{\upsilon} = \mathbf{v}+\mathbf{w}$, $\mathbf{v} := \nabla\Phi$, $\nabla\cdot\mathbf{w} = 0$, because $\eta\nabla\times\nabla\times\boldsymbol{\upsilon} = -\eta\Delta\mathbf{w}$, then for decompositions $\mathbf{w} = \mathbf{w}^{(1)}+\mathbf{w}^{(2)}+o^2$, $\mathbf{w}^{(1)}$ fulfills equation $(\Delta+k_s^2)\widehat{\mathbf{w}}^{(1)}(\mathbf{x},\omega) = 0$, $\widehat{\mathbf{w}}^{(1)} = F[\mathbf{w}^{(1)}]$; $k_s := (1+i)/\delta_s$ and $\delta_s := \sqrt{2\eta/\omega}$ are normalized counterparts of k_s', δ_s'. If $\eta \ll 1$, then wave length is much larger than the boundary layer thickness. In our case $\mathbf{w}^{(1)}$ is restricted to thin boundary layer of thickness $\delta_s \sim r_0/16$ ($r_0' = 2$ μm, $\omega' = 20$ MHz). Also the amplitude corrections brought by this force are evaluated as of order δ_s/r_0 (Settnes, Bruus, 2012). It means that direct interactions do not occur additionally $\langle\mathbf{w}^{(1)}\rangle = \mathbf{0}$. In the second order $\mathbf{w}^{(2)}$ is the non-linear reaction of the medium to the disturbance $\mathbf{w}^{(1)}$ and $\widetilde{P}$. $\langle\mathbf{w}^{(2)}\rangle$ is the speed of streaming where component z corresponds to v_z given in introduction. This is a secondary effect in $\boldsymbol{\Pi}$, depending on the acoustic excitation. The case $\mathbf{w}^{(1)}$ is not obvious because it is the first order in relation to the acoustic field. Although in our case $\mathbf{w}^{(1)}$ is small ($\delta_s/r_0 \ll 1$), it is not always the case. Obviously, $\mathbf{w}$ has the correct components inside the inclusions. For fluid inclusions, they are omitted in the determination of ADF (ARF) for the same reason as external $\mathbf{w}^{(1)}$. The $\langle\mathbf{w}^{(2)}\rangle \neq 0$ represents inner micro streaming unlike Eckhart's flow. For solid inclusions, inner stationary flow does not exist. It is replaced by second-order stationary shape-deforming stresses that can be completely neglected.

From above reasons for ADF density we have $\nabla\circ\langle\boldsymbol{\Pi}\rangle = -\nabla\langle\widetilde{P}\rangle$. For perturbation solutions of Eqs (1)–(4), in potential approximation, $\Phi = \Phi^{(1)}+\Phi^{(2)}+o^2$, $\widetilde{P} = P^{(1)}+P^{(2)}+o^2$, where $\mathbf{v} = \mathbf{v}^{(1)}+o = \nabla\Phi^{(1)}+o$, we get $P^{(1)} = -g\partial_t\Phi^{(1)}$, where:

$$P^{(2)} = -g\partial_t\Phi^{(2)} - q\frac{g}{2}\left(\left(\mathrm{v}^{(1)}\right)^2 - \left(\frac{P^{(1)}}{gc}\right)^2\right) + o^2, \qquad (6)$$

$$\left(\mathrm{v}^{(1)}\right)^2 := \mathbf{v}^{(1)}\cdot\mathbf{v}^{(1)}.$$

The acoustical pressure is given by $P = P^{(1)} - g\partial_t\Phi^2$ and for periodical disturbances $\langle P\rangle = 0$.
For the Fourier's representation of disturbances

$$P^{(1)}(\mathbf{x},t) = \frac{1}{2}\sum_{\omega}C(\mathbf{x},\omega)e^{-i\omega t} + c.c, \qquad (7)$$

$$\mathbf{v}^{(1)}(\mathbf{x},t) = \frac{1}{2}\sum_{\omega=0}\mathbf{u}(\mathbf{x},\omega)e^{-i\omega t} + c.c,$$
$$\mathbf{u}(\mathbf{x},\omega) = \frac{\nabla C(\mathbf{x},\omega)}{i\omega g}. \qquad (8)$$

For mean value of $\widetilde{P}$ we obtain:

$$\langle\widetilde{P}\rangle = -q\frac{g}{4}\sum_{\omega}\left(|\mathbf{u}|^2 - \frac{1}{(gc)^2}|C|^2\right). \qquad (9)$$

3. Scattered field determination

To determine Eq. (9), it is necessary to determine the acoustic field, in particular in the neighborhood of heterogeneity. Usually solutions for a scattered field are sought in the form of infinite series of functions that satisfy the wave equations in homogeneous phases of the medium and appropriate boundary conditions at the interface (inclusions). These series are slowly converging which causes a number of difficulties in theoretical analysis. We can limit ourselves to one or two terms of a series in the case of extremely asymptotic relations between the parameters determining the

course of the phenomenon. We use an approach based on the integral formulation of the problem of scattering. It allows for considerable flexibility in the methods of searching for and presenting analytical and numerical solutions, including approximations with a simpler analytical structure, however, sufficient or very accurate.

In our model of the heterogeneous medium (suspension) we assume that the reference homogeneous medium surrounds J space volumes ϑ_j. Each region ϑ_j is filled with medium and their homogeneous density $g_j \neq g_0 = 1$, speed of the sound waves $c_j \neq c_0 = 1$ and absorption coefficient $a_j(\omega) \neq a_0(\omega)$, $a_0(\omega)$ are normalized absorption coefficient of the ambient medium, $a(\omega) = \mathrm{F}[\boldsymbol{\mathcal{A}}]$, $\mathrm{F}[\cdot]$ is the Fourier transform, $\boldsymbol{\mathcal{A}} \coloneqq \boldsymbol{\mathcal{A}}^v \nabla$ (Wójcik, Gambin, 2017). Material parameter (density) distributions are given by:

$$g(\mathbf{x}) = g_0 + \sum_{j=1}^{J} [g_j - g_0]\, \chi_j, \tag{10}$$

where $\chi_j \coloneqq \chi(\vartheta_j)$ is the characteristic function of ϑ_j, and analogously for the other parameters.

In heterogeneous lossy medium C satisfies Sturm-Liouville equation (perturbed Helmholtz). By converting this equation into an integral equation of a scattered field, we get (Wójcik *et al.*, 2011; Brekhovskikh, Godin, 1990),

$$C^S(\omega,\mathbf{x}) + k_0(\omega)^2 \int\limits_{\vartheta(\mathbf{x}')} G(\mathbf{x}-\mathbf{x}') W(\mathbf{x}', \nabla_{\mathbf{x}'}) C^S(\omega,\mathbf{x}')\, \mathrm{d}\vartheta$$
$$= -k_0(\omega)^2 \int\limits_{\vartheta(\mathbf{x}')} G(\mathbf{x}-\mathbf{x}') W(\mathbf{x}', \nabla_{\mathbf{x}'}) C^I(\omega,\mathbf{x}')\, \mathrm{d}\vartheta, \tag{11}$$

where $G(\omega,\mathbf{x}) \coloneqq \exp(ik(\omega)\,|\mathbf{x}|)/4\pi\,|\mathbf{x}|$ is the Green function of the Helmholtz equations, $\vartheta \coloneqq \cup\vartheta_j$, $C^S \coloneqq C - C^I$ is the scattering field, C is the total field in the medium, C^I is the incident field, $W(\mathbf{x},\nabla) \coloneqq V(\mathbf{x}) + \nabla\Gamma(\mathbf{x})\cdot\nabla$ is the scattering potential. For our model Eq. (10), $W(\mathbf{x},\nabla) \coloneqq \sum\limits_{j=1}^{J} W_j(\mathbf{x},\nabla)$, $W_j(\mathbf{x},\nabla) \coloneqq V_j\chi_j(\mathbf{x}) + (1/k_0(\omega)^2)\Gamma_j\nabla\chi_j(\mathbf{x})\cdot\nabla$, where:

$$\begin{aligned} V_j &\coloneqq \left(1 - \frac{c_0^2(1+2ia_j(\omega)/k_j)}{c_j^2\,(1+2ia_0(\omega)/k_0)}\right), \\ \Gamma_j &= \frac{g_j - g_0}{(g_j+g_0)/2}, \end{aligned} \tag{12}$$

$$\begin{aligned} k_0^2 &\coloneqq \frac{\omega^2}{c_0^2}\left(1 + 2i\frac{a_0(\omega)c_0}{\omega}\right), \\ k_j^2 &\coloneqq \frac{\omega^2}{c_j^2}\left(1 + 2i\frac{a_j(\omega)c_j}{\omega}\right). \end{aligned} \tag{13}$$

For one-component suspension, it is reasonable to assume that all V_j, Γ_j are identical or can be represented by average values V, Γ. For simplification further calculations will be made for spherical scatterers with mean size $r_0 = \langle r_{0j}\rangle_j$ and volume $\vartheta_0 \coloneqq 4\pi r_0^3/3$. We assume that:

1) for individual scatterer the condition for applying of the single scattering approximation is mean $2\cdot\|W\|\cdot(k_0(\omega)\cdot r_0)^2 \ll 1$, where $\|W\| = \max\limits_{\mathbf{x},j}|W_j|$ is the norm of the scattering potential;
2) the contribution of multiply scattered field on the other scatterers to the ADF of the single scatterer can be omitted. The results of the work (Wójcik *et al.*, 2011) showed that the cross-sections for scattering in the second order are several dozen times smaller than in the first order.

Additionally, absorption of the ambient medium further attenuates this relationship. A stochastic medium with large $\|W\|$ was considered, scatterers were located at distances comparable to their sizes and are sonicated by waves of comparable (with scatterers dimension) wavelength.

Let vector $\mathbf{R}_j = (z_j, x_j, y_j) = \left(z_j, \boldsymbol{\rho}_j\right)$, $R_j = |\mathbf{R}_j|$ describe space position of fixed point inside volume ϑ_j, introducing new vector variable $\boldsymbol{\xi} = \mathbf{x}' - \mathbf{R}_j$, $\nabla_{x'} = \nabla_\xi$, and $\mathbf{r} = \mathbf{x} - \mathbf{R}_j$. In the vicinity of the point $\mathbf{R}_j$ of the small particles the incident "transducer" field may be presented as the locally plane, $C^I(\omega,\mathbf{x}') = C^I(\omega,\mathbf{R}_j + \boldsymbol{\xi}) \cong C^I(\omega,\mathbf{R}_j)e^{i\mathbf{k}_I(\omega)\cdot\boldsymbol{\xi}}$, where for example, $C^I(\omega,\mathbf{R}_j) \coloneqq C_0(\omega)2\partial_{z'} \int\limits_{\mathbf{x}_\sigma\in\sigma} G(\mathbf{R}_j - \mathbf{x}_\sigma + \boldsymbol{\xi})\, \mathrm{d}\sigma$ is the field satisfying Dirichlet boundary conditions, emitted by plane uniformly apodised, perpendicular to z axis transducer. For plane wave $C^I(\omega,\mathbf{R}_j) \coloneqq C_0(\omega)e^{i\mathbf{k}_I(\omega)\cdot\mathbf{R}_j}$. $C_0(\omega)$ is transmitted pulse Fourier spectrum, $\mathbf{k}_I(\omega) = k_0(\omega)\mathbf{e}_I$, $\mathbf{e}_I$ is the unit vector in the direction of the plane wave propagation, $k(\omega) \cong \omega + ia_0(\omega)$. For transducer $\mathbf{e}_I = \mathbf{R}_j/R_j$, σ is the transducer surface. Using above expansion in Eq. (11) we obtain field scattered by single scatterer,

$$C_j^S(\omega,\mathbf{R}_j+\mathbf{r}) = -k_0(\omega)^2 C^I(\omega,\mathbf{R}_j) \int\limits_{\vartheta_j(\xi)} G(\omega,\mathbf{r}-\boldsymbol{\xi})$$
$$\cdot W_j(\boldsymbol{\xi},\nabla_\xi)e^{i\mathbf{k}_I(\omega)\cdot\boldsymbol{\xi}}\, \mathrm{d}\vartheta. \tag{14}$$

Equation (14) can be easily numerically calculated. Because $k\xi^2/2r \leq kr_0/2 \ll 1$ for $r \geq r_0$, $\xi = |\boldsymbol{\xi}|$, $r = |\mathbf{r}|$, then in the Green function expansion $G(\omega,\mathbf{r}-\boldsymbol{\xi}) \cong G(\omega,\mathbf{r})\cdot\exp(-i\mathbf{k}_s(\omega)\cdot\boldsymbol{\xi})$ Fresnel terms may be omitted. Moreover, obtained formulas may be used (as Eq. (14)) for determination of the field on the heterogeneity surface. $\mathbf{k}_s(\omega) \coloneqq k_0(\omega)\mathbf{e}_s$ is the wave vector of scattering wave, $\mathbf{e}_S = (\mathbf{x}-\mathbf{R}_j)/|\mathbf{x}-\mathbf{R}_j| = \mathbf{r}/r$. Applying above approximation in Eq. (14) we get:

$$C_j^S(\omega,\mathbf{x}) = -k_0(\omega)^2 C^I(\omega,\mathbf{R}_j) G(\omega,\mathbf{x}-\mathbf{R}_j)$$
$$\cdot \widehat{W}_j(\mathbf{k}_S - \mathbf{k}_I, \mathbf{k}_I), \tag{15}$$

where

$$\widehat{W}_j(\mathbf{k}_S-\mathbf{k}_I,\mathbf{k}_I) := \int\limits_{\vartheta_j(\boldsymbol{\xi})} \mathrm{e}^{-i\mathbf{k}_S\cdot\boldsymbol{\xi}} W_j(\boldsymbol{\xi},\nabla_\xi)\mathrm{e}^{i\mathbf{k}_I(\omega)\cdot\boldsymbol{\xi}}\,\mathrm{d}\vartheta = \left(V+(1/k_0^2)(\mathbf{k}_S-\mathbf{k}_I)\cdot\mathbf{k}_I\Gamma\right) \cdot\widehat{\chi}_j(\mathbf{k}_S-\mathbf{k}_I), \tag{16}$$

$\widehat{\chi}_j(\mathbf{k}_S-\mathbf{k}_I) = \mathrm{F}\left[\chi_j(\boldsymbol{\xi}),\mathbf{k}_S-\mathbf{k}_I\right] = \widehat{\chi}_j\left(k_0(\omega)(\mathbf{e}_S-\mathbf{e}_I)\right)$ is the space Fourier transform of $\chi_j(\boldsymbol{\xi})$.

In the spherical system of coordinates centered at $\mathbf{R}_j$, oriented respect direction $\mathbf{e}_I$ of incident wave $\mathbf{e}_S\cdot\mathbf{e}_I = \cos(\theta)$, $\mathbf{r} = (r\cos(\theta), r\sin(\theta)\cos(\varphi), r\sin(\theta)\sin(\varphi))$, $\mathbf{k}_I\cdot\mathbf{r} = kr\cos(\theta)$, the total field $C_j = C_j^I + C_j^S = C_j(\omega,\mathbf{R}_j+\mathbf{r})$ in vicinity of the spherical heterogeneity of radius r_0 takes the form

$$C_j(\omega,\mathbf{R}_j,r,\theta) = C^I(\omega,\mathbf{R}_j)H(r,\theta,\omega), \tag{17}$$

$$H(r,\theta,\omega) := \left(e^{ik_0(\omega)\cdot r\cos(\theta)} - k_0(\omega)^2\frac{e^{ik_0(\omega)r}}{4\pi r}\widehat{W}(\theta,r_0)\right), \tag{18}$$

where

$$\widehat{W}_j(\theta,r_0) = \vartheta_0\cdot(V+(\cos(\theta)-1)\Gamma) \cdot f\left(2r_0k_0(\omega)\sin(\theta/2)\right),$$
$$f(\cdot) := 3\left(\sin(\cdot)-(\cdot)\cos(\cdot)\right)/(\cdot)^3.$$

4. Forces determination

The velocity components $\mathbf{u}_j(\omega,r,\theta) = (u_r,u_\theta,0)_j$ are calculated on the basis of Eqs (8) and (17):

$$|\mathbf{u}_j|^2 = \left|C^I(\omega,\mathbf{R}_j)\right|^2|\mathbf{U}(r,\theta,\omega)|^2\Big/(g_0c_0)^2, \tag{19}$$

$$|\mathbf{U}(r,\theta,\omega)|^2 := \left(|\partial_r H|^2+|\partial_\theta H/r|^2\right)\Big/k_0^2. \tag{20}$$

Substituting Eqs (17) and (19) into Eq. (9) then into Eq. (5) and integrating in a spherical coordinate system, $\mathbf{n} = \mathbf{r}/r = \mathbf{e}_S$, $\mathrm{d}s = r_0^2\sin(\theta)\,\mathrm{d}\theta\,\mathrm{d}\varphi$ we get:

$$\mathbf{F}_j = q\frac{\pi r_0^2}{2g_0c_0^2}\sum_\omega\left|C_j^I\right|^2Q(\omega,r_0)\mathbf{e}_I, \tag{21}$$

$$Q(\omega,r_0) := \int\limits_0^\pi\left(|\mathbf{U}|^2-|H|^2\right)_{r=r_0}\cos(\theta)\sin(\theta)\,\mathrm{d}\theta. \tag{22}$$

From Eqs (12), (16) and (22) it follows that $\mathbf{F}_j$ can change the sign relative to $\mathbf{e}_I$ or at the transition from $g_j > g_0 = 1$ or $c_j > c_0 = 1$ to $g_j < 1$ or $c_j < 1$, respectively. In our case, for capsule SF6 $Q(\omega,r_0) < 0$.

Let us consider, for simplicity and also from experimental reasons, cylinder (or cylindrical shell) of the base area S_c, length l_c, volume $\vartheta_c = S_c\cdot l_c$, $\vartheta_c \gg \vartheta_0$ and axis parallel to $\mathbf{e}_I = (1,0,0)$ unit vector in direction of the incident plane wave. Let cylinder be positioned between z_c and z_c+l_c planes. Because $i\mathbf{k}_I\cdot\mathbf{R}_j + c.c = -2a_0(\omega)z_j$, $z_j = z_c+\delta z_j$, $0\le\delta z_j\le l_c$, then the sum of the driving forces acting on $J = \beta\vartheta_c$ suspension particles in volume ϑ_c is proportional to:

$$\sum_{j=1}^J\left|C_j^I\right|^2 = |C_0|^2\,e^{-2a_0(\omega)z_c}\sum_{j=1}^J e^{-2a_0(\omega)\delta z_j}. \tag{23}$$

According to the mean value theorem there exists such δz that the sum on the right hand side in Eq. (23) takes the form $J\exp(-2a_0(\omega)\delta z)$. In stationary flow, spatial distributions of scatterers change from observation to observation (that means that δz fluctuates). Suppose, however, that in a given area they are realizations of the same stationary stochastic process with specific probability densities of random variables δz_j. Assume that these are identical uniform distributions in volume ϑ_c.

After averaging respect this distributions, the total driving Force acting on particles is:

$$\mathbf{F} = qJ\frac{\pi r_0^2}{2g_0c_0^2}\sum_\omega|C_0(\omega)|^2Q(\omega,r_0) \cdot e^{-2a_0(\omega)z_c}\cdot\frac{(1-e^{-2a_0(\omega)l_c})}{2a_0(\omega)l_c}\mathbf{e}_I. \tag{24}$$

In the case of homogeneous absorbing medium the right hand side of Wu and Du model equation, which we gave in introduction, determined density $\mathrm{ADF}_h := (1/c_0)\partial_z I_z\mathbf{e}_I$. Then

$$\mathbf{F}_h \equiv \mathrm{ADF}_h = \mathbf{e}_I(1/c_0)\int\limits_{\vartheta_c}\partial_z I_z d\vartheta_c = \mathbf{e}_I(1/c_0)S_c\left(I_z(z_c+l_c)-I_z(z_c)\right). \tag{25}$$

Because,

$$I_z(z)\cong|C_0(\omega)|^2\exp(-2a_0(\omega)z)/2g_0c_0,$$

then for incident plane wave in the homogenous absorbing medium the driving force for above describing cylindrical volume:

$$\mathbf{F}_h = q\frac{S_c}{2g_0c_0^2}\sum_\omega|C_0(\omega)|^2\,e^{-2a_0(\omega)|z_c|}\left(1-e^{-2a_0(\omega)l_c}\right)\mathbf{e}_I. \tag{26}$$

The relations $\varepsilon := F/F_h$, $F = |\mathbf{F}|$, $F_h = |\mathbf{F}_h|$ are important for this work. It can be easily numerically determined, nevertheless several approaches can be proposed for simplification Eqs (24) and (26) and ε. If the wideband of $|C_0(\omega)|^2$ is narrow or/and $Q(\omega,r_0)$ is slowly varying function respect $|C_0(\omega)|^2$ (it is because is determined in the range of long-wave asymptotic of scattering), then

$$\varepsilon\cong\beta\pi r_0^2Q(\omega_c)\big/2a_0(\omega_c), \tag{27}$$

ω_c is carrier frequency or a frequency of the maximum of $|C_0(\omega)|$. For heterogeneous incident field ("transducer field") we obtain the same results. Corresponding

to Eqs (24) and (26), equations contain additional factors that are equal to each other. This is due to the averaging process of the random variables $\mathbf{R}_j$ (demonstrated above), which "sample" the field in the volume ϑ_c.

5. Numerical calculations

In calculations the transmitting pulse had amplitude $P_0 = 0.225$ MPa, rectangular envelope, consisted of 10 oscillation cycles with frequency $\omega_c'/2\pi = 20$ MHz and met the approximation conditions of Eq. (27). The volume ϑ_c was located in the area of the far field $z_c' = 0.009$ m of the plane transducer beam of diameter 2 mm and in plane wave $K_0' = 2\pi/0.03$ 1/m.

The calculations were made for a starch and capsule suspensions in water for the following data:

1) water: density $g' = 1000\,\mathrm{kg/m^3}$, speed of sound $c' = 1500$ m/s, ($g = g_0 = 1$, $c = c_0 = 1$), coefficient of absorption $a_0'(\omega') = \alpha_2' \cdot (\omega'/2\pi)^2$, $\alpha_2' = 2.54 \cdot 10^{-14}$ Np/mHz^2, $a_0(\omega) = \alpha_2 \cdot \omega^2$, $\alpha_2 = 3.03 \cdot 10^{-7}$, kinematic coefficients of shear viscosity $\eta_s' = 10^{-6}$ kg/ms;
2) average starch: density $g' = 1500\,\mathrm{kg/m^3}$, sound speed $c' = 2800\,\mathrm{kg/m^3}$ ($g = 1.5$, $c = 1.87$), radius $r_0' = 2$ μm. The following concentrations were made $\beta_m = \delta\beta \cdot m\delta\beta = 20000$ 1/mm^3, $m = 0, 1, 2, 3, 4$;
3) average capsule BR-14: mean density (lipid + gas) $g' = 25\,\mathrm{kg/m^3}$ ($g = 0.025$), radius $r_0' = 1$ μm, shell density $g_{sh}' = 1260\,\mathrm{kg/m^3}$, speed of sound $c_{sh}' \cong c'$ ($g_{sh} = 1.26$, $c_{sh} \cong 1$), shell thickness $\delta r_{sh}' = 0.005$ μm, gas SF6 density $g_g' = 6.13\,\mathrm{kg/m^3}$, speed of sound $c_g' \cong 120$ m/s, ($g \cong 0.006$, $c_g = 0.08$), coefficient of absorption $a'(\omega'/2\pi) = \alpha_{SF6}'(\omega'/2\pi)^2$, $\alpha_{SF6}' \cong 2.21 \cdot 10^{-10}$ Np/mHz^2. $a'(20\text{ MHz}) \cong 8.8 \cdot 10^4$ Np/m, in normalized units $a_{SF6}(400) = 341$. Sound speed and absorption parameter of SF6 were estimated based on the works (Cannell, Sarid, 1974; Estrada-Alexanders, Hurly, 2008; The Engineering Toolbox, 2008). The following concentrations were made $\beta_m = \delta\beta_b \cdot m$, $\delta\beta_b = 1000$ 1/mm^3, $m = 0, 1, 2, 4$.

Introducing additive components $Q_{\mathbf{U}}$, Q_H and angle density $\delta Q(\omega, r_0, \theta) := \left(|\mathbf{U}|^2 - |H|^2\right)$ of the Q function on the surface $r = r_0$, the Eq. (22) may be rewritten in the form

$$\begin{aligned} Q(\omega, r_0) &= Q_{\mathbf{U}} + Q_H \\ &:= \int_0^{\pi} \left(|\mathbf{U}|^2 - |H|^2\right)_{r=r_0} \cos(\theta)\sin(\theta)\,\mathrm{d}\theta \\ &= \int_0^{\pi} \delta Q(\omega, r_0, \theta)\sin(\theta)\cos(\theta)\,\mathrm{d}\theta. \end{aligned}$$

As we see on the sphere surface

$$\left\langle \widetilde{P}(\omega, r_0, \theta)\right\rangle \propto -\delta Q(\omega, r_0, \theta)$$

and force density

$$\delta \mathrm{F}(\omega, r_0, \theta) =\propto \delta Q(\omega, r_0, \theta)\sin(\theta)\cos(\theta).$$

Angle distributions of $\langle \widetilde{P}\rangle$ and δF for solid (starch) and gaseous (SF6) heterogeneities are presented in Figs 1 and 2, respectively. Fourier spectrum of Q and their "velocity" $Q_{\mathbf{U}}$ and "pressure" Q_H components for solid and gaseous heterogeneities are in Figs 3a and 3b.

The resonant frequencies of the BR14 capsules are located in the vicinity of 6 MHz. It was assumed that it is not a secondary source of acoustic field. Due to the small volume fraction of the shell (≅0.015) and similar impedances of the shell and water, $gc = 1.26$ and $g_0c_0 = 1$ respectively, it was assumed that the magnitude of the scattering potential of the capsule is determined by the speed of sound and absorption in SF6 (see Eq. (12)). Although the compressibility of the gas is many times greater than the shell, the compressibility $\kappa := 1/(gc^2)$ (stiffness gc^2) of the lipid shell which closes the gas, decides on the compressibility of the capsule as the whole.

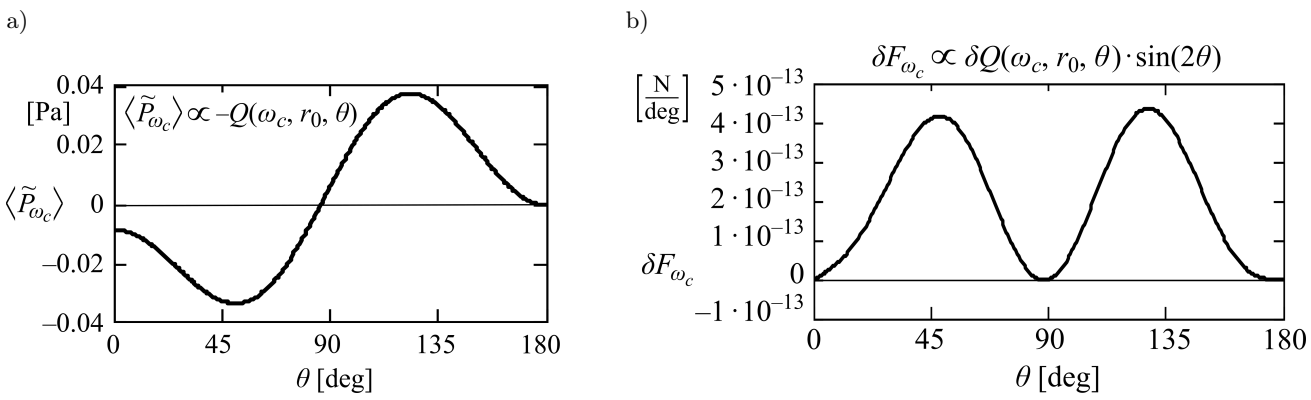

Fig. 1. Starch. Surface distributions of the Fourier component $\omega_c' = 20$ MHz: (a) of the mean pressure $\langle \widetilde{P}_{\omega_c}\rangle$, (b) of the angle force density $\delta \mathrm{F}_{\omega_C}$.

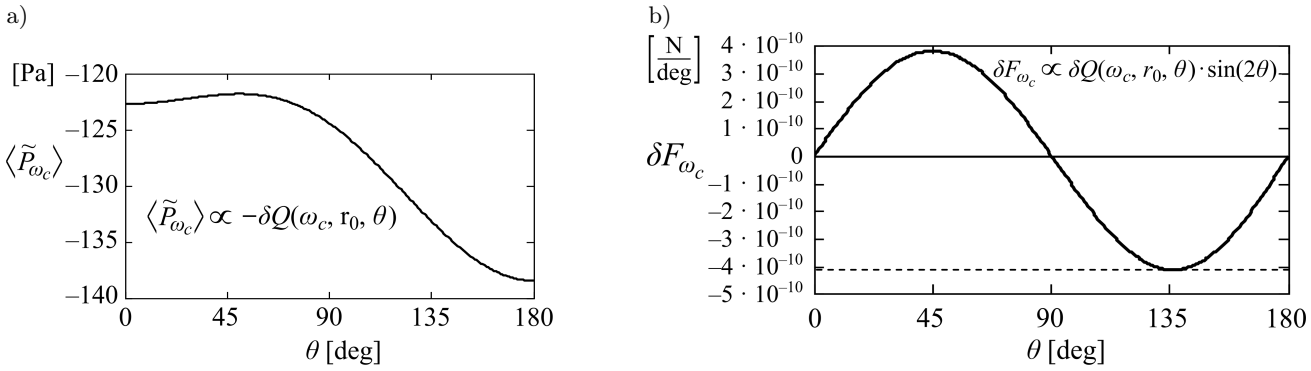

Fig. 2. Gas. Surface distributions of the Fourier component $\omega_c' = 20$ MHz: a) of the mean pressure $\langle \widetilde{P}_{\omega_c} \rangle$, b) of the angle force density $\delta \mathrm{F}_{\omega_C}$.

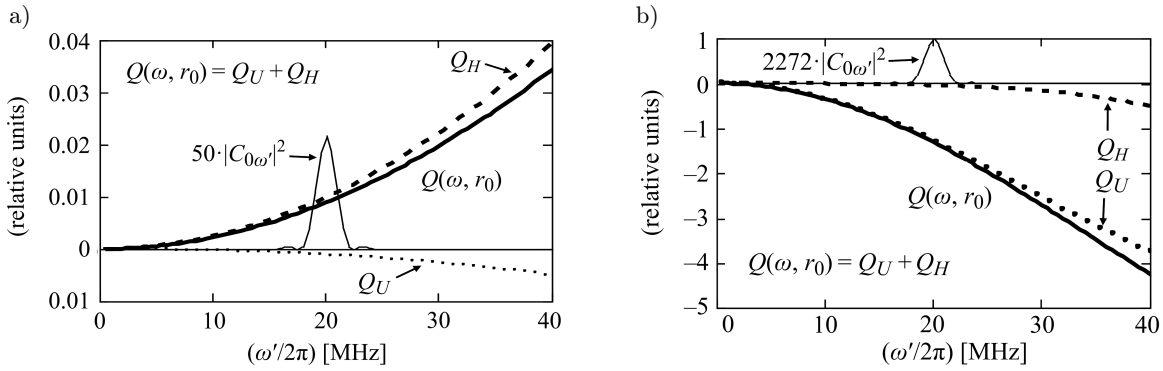

Fig. 3. Dependence of the Q function – continuous bold lines and their components, Q_H – dashed and $Q_{\mathbf{U}}$ – doted lines, on the frequency for the starch (a) and for capsule with the SF6 (b). Amplified of the transmitted pulse $|C_{0\omega'}|^2$ – power Fourier spectrum – thin solid line.

For ARF (see comments in Sec. 2)

$$\delta Q(\omega, r_0, \theta) := \left(b_g |\mathbf{U}|^2 - b_\kappa |H|^2 \right),$$

where $b_g := (1 - g/g_0)$, $b_\kappa := (1 - \kappa/\kappa_0)$, $\kappa_0 = 1/g_0 c_0^2 = 1$. Then:

$$Q(\omega, r_0) = b_g Q_{\mathbf{U}} + b_\kappa Q_H. \tag{28}$$

For starch $b_g = -0.5$, $b_\kappa \cong 0.81$. For BR14 capsule $b_g \cong 0.994$ for lipid shell $b_\kappa \cong 0.206$. Bearing in mind the relationship between the plots Q_H and $Q_{\mathbf{U}}$ in Figs 3a and 3b, and values b_g and b_κ which modifying $Q_{\mathbf{U}}$, Q_H and $Q(\omega, r_0)$ accordingly Eq. (28) in the region 20 MHz, we conclude that: in the case of starch (a) the change made by b_κ is significantly compensated by the change made by b_g, in the case of capsule BR14 (b) the change is also small. Below, next to the values for ADF, we give the values corresponding to the ARF obtained after the substitution of Eq. (28) into Eq. (27).

Accordingly, in Eq. (26), the ADF_h acting on 1 mm^3 of water by the unit plane continuous wave is $F_h' = 1.13 \cdot 10^{-7}$ N, but for above described pulsed disturbance, similar to using in experiment, $F_h' = 2.133 \cdot 10^{-9}$ N; $F_h' = F_h \cdot P_0'/K_0'^2$ in dimensional units.

For solid inclusions concentration $\beta_1 = \delta\beta = 20\,000$ 1/mm^3, using exact formula $\varepsilon := F/F_h$ and full wideband of the pulse intensity (see Fig. 3) we obtain, $\delta\varepsilon := \varepsilon(\delta\beta) = 0.112$. In the ARF case $\delta\varepsilon = 0.109$. For approximated Eq. (27), which is equivalent to usage of unit plane continuous wave, $\delta\varepsilon \cong 0.112$. The ADF acting on the one particle bay pulsed disturbance is $F'/J = 1.2 \cdot 10^{-14}$ N. However, ADF in the case of unit plane continuous wave is $F'/J = 6.31 \cdot 10^{-13}$ N.

In the case of bubbles, because of $c_{sh} \cong 1$ and small $\delta r_{sh}'$, it can be shown that influence of the shell on the scattering potential is negligible. It was assumed that $\omega_c'/2\pi$ is outside the bubbles resonance. For bubbles concentration $\beta_1 = \delta\beta_b = 1000$ 1/mm^3, using exact formula $\varepsilon := F/F_h$ and full wideband of the pulse intensity (see Fig. 3) we obtain $\delta\varepsilon = -1.142$. In ARF case, $\delta\varepsilon = 0.137$. For approximation Eq. (27) (plane continuous wave), $\delta\varepsilon \cong -0.145$. The ADF acting on the one bubble bay pulsed disturbance is $F'/J = -3.67 \cdot 10^{-13}$ N. However, ADF in the case of unit plane continuous wave is $F'/J = -1.61 \cdot 10^{-11}$ N. For pulse disturbance, the relations between forces acting on bubble and solid inclusions is approximately equal ~ 31.

6. Experiment

The measurements were done in the aqueous suspension of the corn starch, with material parameters as in point 2 of Sec. 5, and ultrasound contrast bub-

bles with parameters as in Sec. 3. The suspension had blood-like acoustic properties and was used as a blood mimicking liquid (YOSHIDA *et al.*, 2012). The suspensions concentrations of $\beta_m = \delta\beta \cdot m$, $\delta\beta = 20\,000$ 1/mm^3, $m = 0, 1, 2, 3, 4$, were investigated. As a reference liquid, a 0.01 g/l ($\beta_{ref} = 200$ 1/mm^3) aqueous suspension of starch was used. With such a low starch concentration, it was expected that the measured flow velocity would be similar to that of the pure water. This concentration was sufficient to obtain 20 dB Doppler signal-to-noise ratio and to estimate the maximum flow velocity. The direction of the streaming of the reference liquid corresponded to the direction of the acoustic wave propagation. In the next experiment, the streaming velocity of the bubble suspension of the Bracco BR14 (SF6) ultrasonic contrast was measured. Concentrations of$\beta_m = \delta\beta_b \cdot m$, $\delta\beta_b = 1000$ 1/mm^3, $m = 0, 1, 2, 4$, were studied.

A 2 mm diameter, 20 MHz, flat ultrasonic transducer was used to generate the streaming and to measure simultaneously the streaming velocity. The streaming velocity was recorded in a sample volume located 9 mm from the transducer face. The transducer was driven by an ultrasonic Doppler flow meter. The Doppler signal from the output of the pulse flowmeter was recorded by the LeCroy 62Xi digital oscilloscope. $50 \cdot 10^3$ signal samples were recorded in 1 s. Bandwidth was limited to 0–1.45 kHz at −3 dB. A $32 \cdot 10^3$ point FFT with Hamming window were calculated. Doppler spectra in 0–25 kHz frequency range and $\Delta f = 1.5$ Hz resolution were obtained. Next 50 spectra were averaged. For the reference signal 0.01 g/l starch suspension, 1000 spectra were averaged for a 20 dB noise separation. Finally, the maximum Doppler frequency and the maximum streaming velocity was calculated from the Doppler formula $f_d = f_u \cdot (w/c_0')2\cos(\theta)$, where f_d is the Doppler shift frequency, f_u is the ultrasound frequency (20 MHz), w is the streaming velocity, c_0' (= 1500 m/s) is the speed of sound and θ (= 0 rad) is the angle between the flow direction and the propagation direction of the ultrasonic wave.

The spectra of the Doppler signal for the different concentrations of the corn starch suspension are shown in Fig. 4.

The calculated maximum streaming velocities for the recorded spectra are presented in Table 1. The third column contains relative velocity increase of $\delta\varepsilon_m := (v_m - v_{m-1})/v_{\text{ref}}$ and the average relative increase of $\delta\varepsilon_{\text{exp}} := \langle\delta\varepsilon_m\rangle_m = (v_4 - v_{\text{ref}})/4v_{\text{ref}}$ resulting from concentration increase of the streaming velocity ($v_0 = v_{\text{ref}}$), with step changes in concentration of $\delta\beta = \beta_1$ (= 20 000 1/mm^3). These quantities, especially $\delta\varepsilon_{\text{exp}} = 0.107$, correspond to theoretically determined and numerically calculated $\delta\varepsilon = 0.112$. In theory, because of the linear relationship of F and β, $\delta\varepsilon = \delta\varepsilon_m$. Only for $m = 1$, $|\delta\varepsilon - \delta\varepsilon_1| < 0.018$, when for the other cases $|\delta\varepsilon - \delta\varepsilon_m| < 0.005$.

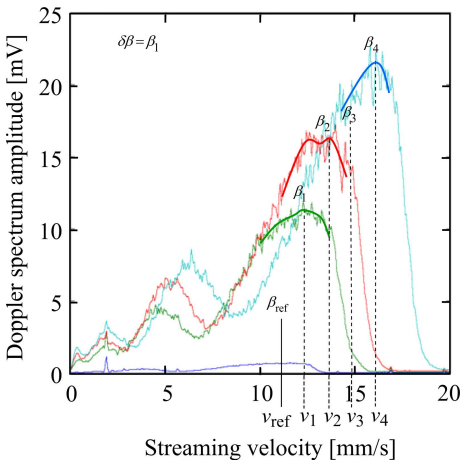

Fig. 4. The maxima of Doppler spectra in the function of the starch concentration $\beta_{(\text{ref},1,2,3,4)}$, and the corresponding streaming velocity $v_{(\text{ref},1,2,3,4)}$. Measured profiles of the spectra-thin lines; locally averaged measured profiles – bold lines.

Table 1. Measured speed of the streaming v_m as a function of starch concentration β_m. Third column – mean relative speed increase $\delta\varepsilon_{\text{exp}}$ and relative speed increase $\delta\varepsilon_m$ as a function of increase of the starch concentration $\delta\beta_m = \beta_m - \beta_{m-1} = \delta\beta = \beta_1$.

Concentrations [1/mm^3]	Velocity [mm/s]	Relative increase $\delta\varepsilon_m := (v_m - v_{m-1})/v_{\text{ref}}$
$\beta_{\text{ref}} = 2 \cdot 10^2$	$v_{\text{ref}} = 11.25$	$\delta\varepsilon_{\text{exp}} := \langle\delta\varepsilon_m\rangle_m = 0.107$
$\beta_1 = 2 \cdot 10^4$	$v_1 = 12.31$	$\delta\varepsilon_1 = 0.094$
$\beta_2 = 4 \cdot 10^4$	$v_2 = 13.63$	$\delta\varepsilon_2 = 0.117$
$\beta_3 = 6 \cdot 10^4$	$v_3 = 14.84$	$\delta\varepsilon_3 = 0.108$
$\beta_4 = 8 \cdot 10^4$	$v_4 = 16.06$	$\delta\varepsilon_4 = 0.109$

The spectra for the Bracco BR14 ultrasonic contrast for different concentration are shown in Fig. 5.

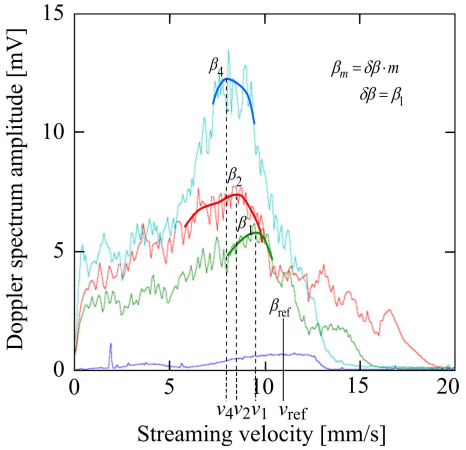

Fig. 5. The maxima of Doppler spectra in the function of the BR14 (SF6 capsule) concentration $\beta_{(\text{ref},1,2,4)}$, and the corresponding streaming velocity $v_{(\text{ref},1,2,4)}$. Measured profiles of the spectra-thin lines while locally averaged – bold lines.

For bubbles, the maximum streaming velocities for the recorded spectra are presented in Table 2.

Table 2. Measured speed of the streaming v_m as a function of starch concentration β_m. Third column – mean relative speed increase $\delta\varepsilon_{\text{exp}}$ and relative speed increase $\delta\varepsilon_m$ as a function of increase of the bubbles concentration $\delta\beta_m = \beta_m - \beta_{m-1} = \delta\beta = \beta_1$.

Concentrations [1/mm^3]	Velocity [mm/s]	Relative increase $\delta\varepsilon_m := (v_m - v_{m-1})/v_{\text{ref}}$
$\beta_{\text{ref}} = 2 \cdot 10^2$	$v_{\text{ref}} = 11.25$	$\delta\varepsilon_{\text{exp}} := \langle\delta\varepsilon_m\rangle_2 \cong -0.125$
$\beta_1 = 1 \cdot 10^3$	$v_1 = 9.5$	$\delta\varepsilon_1 = -0.156$
$\beta_2 = 2 \cdot 10^3$	$v_2 = 8.43$	$\delta\varepsilon_2 = -0.095$
$\beta_4 = 4 \cdot 10^3$	$v_4 = 7.93$	

Due to the rapid loss of proportionality of measured velocity increase as a function of concentration for $m > 2$ (see Fig. 5) only the value given in the table was $\delta\varepsilon_{\text{exp}} := (v_2 - v_{\text{ref}})/2v_{\text{ref}}$. Theoretical value for microcapsules BR14 was $\delta\varepsilon = -0.142$ while the experimental one $\delta\varepsilon_{\text{exp}} = -0.125$. The case $\beta_3 = 3 \cdot 10^3$ was omitted as indistinguishable from β_2 and β_4 (also due to the measuring accuracy of 0.5 mm/s for all cases).

7. Discusion and conclusions

Calculating $\text{ADF}_h + \text{ADF} \to \mathbf{F}_h + \mathbf{F}$ on the basis of Eqs (24) and (26) we obtain

$$\mathbf{F}_h + \mathbf{F} = q\vartheta_c \sum_{\omega} \left(2a_0(\omega) + \beta\pi r_0^2 Q(\omega, r_0)\right) I_z(\omega, z)/c. \quad (29)$$

This along with the experimental results seems to confirm the hypothesis presented in the introduction with regard to suspensions generating a positive Q and within the range of the concentrations used. Experiments with BR14 (negative Q) are much more difficult due to their short lifespan and the inability to use large concentrations (significant costs). It should be noted that in this case the spectra and the corresponding velocities must initially be interpreted only as BR14 bubble streaming velocity, but not the velocity of the mixture with the surrounding fluid. The velocity of the bubbles relative to the detector is positive (in a steady state), however it is negative in relation to surrounding fluid. The ADF_h force acting on the surrounding fluid is positive. So the negative ADF force acts on the bubbles and is directed opposite to force driving the ambient liquid, which is consistent with the predictions of the theory and calculations.

On the other hand, for this reason a significant "capture" and destruction of the BR14 microcapsules by the transducer especially before the setting up of the streaming should be expected. In the description of the local movement of a single microcapsule, its velocity is determined by the balance between Stokes driving force F_{Sto} and the negative ADF generated on the microcapsule $F_{\text{Sto}} \equiv 12\pi\eta_s' g_0' r_0' \delta v = -F'/J$, where δv is the difference of the velocity of the fluid (water) flowing around the bubble and the velocity of the bubble. Using the results of the numerical calculations of $F'/J = -3.67 \cdot 10^{-13}$ N a relative velocity equilibrium $\delta v \cong 0.01$ mm/s can be obtained (it is much less than measurement accuracy). On this basis, for the purposes of interpretation, despite the initial reservations, we assume the equality of the velocity of both phases of the mixture. Increasing the concentration of BR14 from β_1 to β_2 causes a further clear decrease of the bubble velocity (mixture). However, this is not a change as proportional as in the case of starch suspension. Nevertheless $|\delta\varepsilon - \delta\varepsilon_{\text{exp}}| < 0.02$ and it allows us to assume that in the range of the concentration change to β_2 the velocity changes are proportional and satisfactorily agree with the theory. In the experiment, above concentration β_2, we observe a violent collapse of the principle of proportional velocity increase. According to theory, the relative change of velocity for $\beta_4 = 4000$ 1/mm^3 should be equal to -0.57. The value calculated on the basis of the experiment is $\cong -0.3$. The reasons for this disproportion is not recognized yet. We suppose that it can be seen in the disappearance of bubble concentration in relation to the given or more complicated course of the phenomenon than described in the presented theory. For example, the faster the increase of the nonlinearity in relation to the concentration in the case of negative and large ADF. We note that the theoretically calculated force corresponding to the concentration of BR14 of $\beta_4 = 4000$ 1/mm^3 corresponds to the absolute force value for starch concentration of 120 000 1/mm^3.

Nevertheless, experiment and theory showed the possibility of effective control of the movement of suspensions of ultrasound, contrasts and capsules containing drugs and the dependence of the direction of force on the relative values of material parameters.

Acknowledgments

This investigation was supported by NCN grant 2014/15/B/ST8/04345.

References

1. Brekhovskikh L.M., Godin O.A. (1990), *Acoustics of Layered Media I: plane and quasi-plane waves*, Chapter 1, par. 1, Berlin: Springer-Verlag, Berlin, Heidelberg.
2. Cannell D.S., Sarid D. (1974), *Sound propagation in SF6 near the critical point*, Physical Review A, **10**, 6, 2280–2289.
3. Czyz H., Gudra T. (1992), *Forces due to diffraction of sound wave on small diameter cylindrical, particles*, Journal de Physique IV Colloque, **2**, C1, 741–744, doi: 10.1051/jp4:19921161.
4. Eckart C. (1948), *Vortices and streams caused by sound waves*, Physical Review, **73**, 68–76.

5. Estrada-Alexanders A.F., Hurly J.J. (2008), *Kinematic viscosity and speed of sound in gaseous CO, CO_2, SiF_4, SF_6, C_4F_8, and NH_3 from 220 K to 375 K and pressures up to 3.4 MPa*, Journal of Chemical Thermodynamics, **40**, 2, 193–202, doi: 10.1016/j.jct.2007.07.002.
6. Lei J., Glynne-Jones P., Hill M. (2013), *Acoustic streaming in the transducer plane in ultrasonic particle manipulation devices*, Lab on a Chip, **13**, 2013, 2133–2143, doi:10.1039/c3lc00010a.
7. Mitri F.G. (2012), *Interaction of an Acoustical Quasi-Gaussian Beam With a Rigid Sphere: Linear Axial Scattering, Instantaneous Force, and Time-Averaged Radiation Force*, IEEE Transactions on Ultrasonics, Ferroelectrics, and Frequency Control, **59**, 10, 2347–2351, doi: 10.1109/TUFFC.2012.2460.
8. Nowicki A., Kowalewski T., Secomski W., Wójcik J. (1998), *Estimation of acoustical streaming: theoretical model, Doppler measurements and optical visualization*, European Journal of Ultrasound, **7**, 73–81.
9. Nowicki A., Secomski W., Wójcik J. (1997), *Acoustic streaming: comparison of low amplitude linear model with streaming velocities measured by means of 32 MHz Doppler*, Ultrasound in Medicine and Biology, **23**, 5, 783–91.
10. Settnes M., Bruus H. (2012), *Forces acting on a small particle in an acoustical field in a viscous fluid*, Physical Review E, **85**, article ID: 016327, doi: 10.1103/PhysRevE.85.016327.
11. The Engineering Toolbox (2008), *Gases – Speed of Sound*, available at: https://www.engineeringtoolbox.com/speed-sound-gases-d_1160.html/.
12. Tjotta S. (1959), *On some non-linear effects in sound fields with special emphasis on generation of vorticity and the formation of streaming patterns*, Archiv for Mathematik og Naturvidenskab, **55**, 1–68.
13. Wójcik J., Gambin B. (2017), *Theoretical and numerical aspects of nonlinear reflection – transmission phenomena in acoustics*, Applied Mathematical Modelling, **42**, 100–113, doi: 10.1016/j.apm.2016.10.026.
14. Wójcik J., Litniewski J., Nowicki A. (2011), *Modeling and analysis of multiple scattering of acoustic waves in complex media: Application to the trabecular bone*, Journal of the Acoustical Society of America, **130**, 4, 1908–1918, doi: 10.1121/1.3625285.
15. Wu J., Du G. (1993), *Acoustic streaming generated by focused Gaussian beam and finite amplitude tone burs*, Ultrasound in Medicine and Biology, **19**, 2, 167–176.
16. Yoshida T. *et al.* (2012), *Blood-mimicking fluid for the Doppler test objects of medical diagnostic instruments*, 2012 IEEE International Ultrasonics Symposium, doi: 10.1109/ULTSYM.2012.0403, 1–4.
17. Zarembo L.K., Krasilnikow W.A. (1966), *Introduction to Nonlinear Acoustics* [in Russian], Nauka, Moscow.
18. Zhang D.Z., Prosperetti A. (1994), *Averaged equations for inviscid disperse two-phase flow*, Journal of Fluid Mechanics, **267**, 185–219.
19. Zhang D.Z., Prosperetti A. (1997), *Momentum and energy equations for disperse two-phase flows and their closure for dilute suspensions*, International Journal of Multiphase Flow, **23**, 3, 425–453.